Theoretical suggestion for experimental detection of magnetism in atomic clusters by photon scattering

Mogus Mochena
Department of Physics, Florida A&M University, Tallahassee, Florida 32307

A. K. Rajagopal and O. J. Glembocki
Naval Research Laboratory, Washington, DC 20375-5320

(Received 19 August 1998)

We suggest that the large magnetic moments carried by atomic clusters of manganese (for example, 25 bohr magnetons for Mn_5 cluster) may be detected by means of polarized optical spectroscopic methods even on a semiconducting substrate. Our estimate for the magnetic part of the cross section for Mn_5 cluster is of the order of 10^{-6}, including possible resonance contribution from states near the highest occupied molecular orbital state of the cluster. This appears to be well within the accuracy of current spectroscopic techniques. [S0163-1829(99)50402-5]

Ever since the first suggestion by Platzman and Tzoar[1] almost three decades ago that magnetic structures may be experimentally observed by means of x-ray scattering (synchrotron radiation), much progress has been made in making this a quantitative tool in experimentally studying a variety of magnetic structures such as spiral, antiferromagnetic, and ferromagnetic spin arrangements on crystal lattices. This is largely due to the subsequent experimental and theoretical works of de Bergevin and Brunel,[2] and Blume and Gibbs.[3] For a comprehensive account of this work and its applications to magnetism of bulk systems, one may refer to the recent book of Balcar and Lovesey.[4] In the last decade or so, nanostructure materials[5,6] and clusters of atoms[7] have been shown to exhibit various geometric structures and more importantly of current interest, unusually large magnetic moments. Most recently, direct observation of magic clusters which are special sizes of clusters with enhanced stability, has been reported[8] where the clusters were formed on a substrate of silicon (111) surface.

In Ref. 7, the possibility of magnetism and associated geometrical structures of clusters of Mn and MnO in free space was theoretically investigated. The authors found large magnetic moments for cluster sizes of five to ten atoms. In particular, they found Mn clusters up to five atoms retain their atomic magnetic moments (Mn_5 acts as a single unit and carries a magnetic moment of $25\mu_B$). MnO clusters up to nine complexes exhibit similar large moments but depend on geometric structure of the cluster. Concomitantly the magnetic scattering cross section from such clusters is expected to be quite significant, being proportional to the square of the magnetic moment. These estimates of magnetic moments for the free standing clusters may be expected not to change too much when the clusters are deposited on a semiconductor substrate, such as Si(111). The choice of Si(111) was based on lowest dangling-bond density so that the magnetic structure of the Mn clusters may be expected to be least affected. Moreover, there is a recent theoretical calculation of a study of Mn clusters on Ag(001) substrate;[9] the results reported therein suggests other possibilities. In view of the accuracy of their calculations and the remark on the electronic structure of Si(111) mentioned above, it is suggestive that our anticipation may be a reasonable one. In principle, one expects changes in the geometry and magnetic structure of the clusters when the clusters are deposited on a substrate. Only when the magnetic clusters have large magnetic moments when formed on a substrate we would have interesting possibilities for practical application of such systems. The reader should note this caveat concerning the magnetic structure of clusters formed on semiconductor surfaces. In view of the growing interest in processing such large magnetic moments in some novel magnetic device structures,[10] it is of importance to first determine experimentally if these clusters indeed carry such large magnetic moments. While magnetic force microscopy has been used to image implanted much larger numbers of Mn atoms in the presence of a magnetic field,[6] or use of scanning tunneling microscope to study geometrical features of magic structures,[8] it seems essential to find an experimental method for determining the magnetism of clusters *per se* of the type predicted theoretically in Ref. 7. In this paper we suggest a direct optical method for detecting such phenomena, arising out of the earlier work.[2,3] This method in conjunction with other methods such as synchrotron radiation, electron spin resonance,[11] superconducting quantum interference device magnetometry,[12] etc. (most of which have so far examined clusters in rare-gas matrices) will provide additional support to clear experimental determination of magnetic behavior of supported magnetic cluster systems.

We begin by recalling the expression for the cross section for scattering of photons (x rays) from an initial state $|k\lambda\rangle$ to a final $|k'\lambda'\rangle$ by a magnetic structure as worked out in Refs. 2 and 3:

$$\left.\frac{d^2\sigma}{d\Omega' dE}\right|_{\substack{\lambda\to\lambda' \\ a\to b}} = \left[\frac{e^2}{mc^2}\right]^2 \delta(E_a - E_b - \hbar\omega_{k'} + \hbar\omega_k) \times \left| \left\langle b \left| \sum_j e^{i\mathbf{K}\cdot\mathbf{r}_j} \right| a \right\rangle \hat{\boldsymbol{\varepsilon}}_\lambda \cdot \hat{\boldsymbol{\varepsilon}}_{\lambda'} - \frac{i\hbar\omega_k}{mc^2} \times \left\langle b \left| \sum_j e^{i\mathbf{K}\cdot\mathbf{r}_j} \left[\frac{i(\mathbf{K}\times\mathbf{P}_j)\cdot\mathbf{C}_{\lambda\lambda'}}{\hbar k^2} + \mathbf{S}_j \cdot \mathbf{B}_{\lambda\lambda'} \right] \right| a \right\rangle \right|^2, \quad (1)$$

where $\mathbf{B}_{\lambda\lambda'}=\hat{\boldsymbol{\varepsilon}}_{\lambda'}\times\hat{\boldsymbol{\varepsilon}}_{\lambda}+(\hat{\mathbf{k}}'\times\hat{\boldsymbol{\varepsilon}}_{\lambda'})(\hat{\mathbf{k}}'\cdot\hat{\boldsymbol{\varepsilon}}_{\lambda})-(\hat{\mathbf{k}}\times\hat{\boldsymbol{\varepsilon}}_{\lambda})(\hat{\mathbf{k}}\cdot\hat{\boldsymbol{\varepsilon}}_{\lambda'})-(\hat{\mathbf{k}}'\times\hat{\boldsymbol{\varepsilon}}_{\lambda'})\times(\hat{\mathbf{k}}\times\hat{\boldsymbol{\varepsilon}}_{\lambda})$ and $\mathbf{C}_{\lambda\lambda'}=\hat{\boldsymbol{\varepsilon}}_{\lambda'}\times\hat{\boldsymbol{\varepsilon}}_{\lambda}$. Here $|b\rangle$ and $|a\rangle$ are eigenstates of the Hamiltonian of the magnetic system with eigenvalues E_a, E_b, respectively, $\hat{\boldsymbol{\varepsilon}}_{\lambda}$, $\hat{\boldsymbol{\varepsilon}}_{\lambda'}$ are unit vectors of the polarizations of the incoming and outgoing photons with corresponding frequencies ω_k, $\omega_k{}'$, and λ is the index denoting the two polarization directions. $\mathbf{k}$, $\mathbf{k}'$ are the wave vectors (carets on these denote unit vectors) of the incident and scattered photons with $\mathbf{K}=\mathbf{k}-\mathbf{k}'$ their momentum transfer, and $\mathbf{S}$ is the spin-density vector. The sum on j indicates the contributions from all the elements, charge and spin components located at the site j, which participate in the scattering. The expression (1) can be rewritten using the Fourier transforms of the charge, spin, and momentum densities:

$$\rho(\mathbf{K})=\sum_j e^{-i\mathbf{K}\cdot\mathbf{r}_j},\ S(\mathbf{K})=\sum_j S_j e^{-i\mathbf{K}\cdot\mathbf{r}_j}\quad\text{and}$$

$$P(\mathbf{K})=\frac{1}{2}\sum_j (P_j e^{-i\mathbf{K}\cdot\mathbf{r}_j}+e^{-i\mathbf{K}\cdot\mathbf{r}_j}P_j) \tag{2}$$

in the form

$$\left.\frac{d^2\sigma}{d\Omega' dE}\right|_{\substack{\lambda\to\lambda'\\ a\to b}} =\left[\frac{e^2}{mc^2}\right]^2\delta(E_a-E_b-\hbar\omega_{k'}+\hbar\omega_k)\left|\langle b|\rho^{\dagger}(\mathbf{K})|a\rangle(\hat{\boldsymbol{\varepsilon}}_{\lambda}\cdot\hat{\boldsymbol{\varepsilon}}_{\lambda'})+\frac{i\hbar\omega_k}{mc^2}\left\langle b\left|\frac{i(\mathbf{P}^{\dagger}(\mathbf{K})\times\mathbf{K})\cdot\mathbf{C}_{\lambda\lambda'}}{\hbar k^2}-\mathbf{S}^{\dagger}(\mathbf{K})\cdot\mathbf{B}_{\lambda\lambda'}\right|a\right\rangle\right|^2. \tag{3}$$

In Eq. (3), using the integral form of the Dirac delta function and statistical ensemble of electron states represented by the density matrix P_a, the cross section for scattering of incident photons of polarization $\hat{\boldsymbol{\varepsilon}}_{\lambda}$ to scattered photons of polarization $\hat{\boldsymbol{\varepsilon}}_{\lambda'}$, may be written in the form ($\omega=\omega_k-\omega_{k'}$)

$$\begin{aligned}\left.\frac{d^2\sigma}{d\Omega' dE}\right|_{\lambda\to\lambda'} &=\left[\frac{e^2}{mc^2}\right]^2\frac{1}{2\pi\hbar}\int_{-\infty}^{\infty}dt e^{-i\omega t}\\ &\times\Bigg\{\sum_a P_a\langle a|\rho(\mathbf{K})\rho^{\dagger}(\mathbf{K},t)|a\rangle(\hat{\boldsymbol{\varepsilon}}_{\lambda}\cdot\hat{\boldsymbol{\varepsilon}}_{\lambda'})^*(\hat{\boldsymbol{\varepsilon}}_{\lambda}\cdot\hat{\boldsymbol{\varepsilon}}_{\lambda'})+\frac{i\hbar\omega_k}{mc^2}\frac{i}{\hbar k^2}\langle a|\rho(\mathbf{K})[(\mathbf{P}^{\dagger}(\mathbf{K},t)\times\mathbf{K})\cdot\mathbf{C}_{\lambda\lambda'}]|a\rangle(\hat{\boldsymbol{\varepsilon}}_{\lambda}\cdot\hat{\boldsymbol{\varepsilon}}_{\lambda'})^*\\ &-\frac{i\hbar\omega_k}{mc^2}\langle a|\rho(\mathbf{K})(\mathbf{S}^{\dagger}(\mathbf{K},t)\cdot\mathbf{B}_{\lambda\lambda'})|a\rangle(\hat{\boldsymbol{\varepsilon}}_{\lambda}\cdot\hat{\boldsymbol{\varepsilon}}_{\lambda'})^*-\frac{i\hbar\omega_k}{mc^2}\frac{i}{\hbar k^2}\langle a|[\mathbf{C}^*_{\lambda\lambda'}\cdot(\mathbf{K}\times\mathbf{P}(\mathbf{K}))]\rho^{\dagger}(\mathbf{K},t)|a\rangle(\hat{\boldsymbol{\varepsilon}}_{\lambda}\cdot\hat{\boldsymbol{\varepsilon}}_{\lambda'})\\ &+\left(\frac{i\hbar\omega_k}{mc^2}\right)^2\frac{1}{\hbar^2k^4}\langle a|[\mathbf{C}^*_{\lambda\lambda'}\cdot(\mathbf{K}\times\mathbf{P}(\mathbf{K}))][(\mathbf{P}^{\dagger}(\mathbf{K},t)\times\mathbf{K})\cdot\mathbf{C}_{\lambda\lambda'}]|a\rangle\\ &+\left(\frac{i\hbar\omega_k}{mc^2}\right)^2\frac{i}{\hbar k^2}\langle a|[\mathbf{C}^*_{\lambda\lambda'}\cdot(\mathbf{K}\times\mathbf{P}(\mathbf{K}))](\mathbf{S}^{\dagger}(\mathbf{K},t)\cdot\mathbf{B}_{\lambda\lambda'})|a\rangle+\frac{i\hbar\omega_k}{mc^2}\langle a|(\mathbf{B}^*_{\lambda\lambda'}\cdot\mathbf{S}(\mathbf{K}))\rho^{\dagger}(\mathbf{K},t)|a\rangle(\hat{\boldsymbol{\varepsilon}}_{\lambda}\cdot\hat{\boldsymbol{\varepsilon}}_{\lambda'})\\ &+\left(\frac{i\hbar\omega_k}{mc^2}\right)^2\frac{i}{\hbar k^2}\langle a|(\mathbf{B}^*_{\lambda\lambda'}\cdot\mathbf{S}(\mathbf{K}))[(\mathbf{P}^{\dagger}(\mathbf{K},t)\times\mathbf{K})\cdot\mathbf{C}_{\lambda\lambda'}]|a\rangle-\left(\frac{i\hbar\omega_k}{mc^2}\right)^2\langle a|(\mathbf{B}^*_{\lambda\lambda'}\cdot\mathbf{S}(\mathbf{K}))(\mathbf{S}^{\dagger}(\mathbf{K},t)\cdot\mathbf{B}_{\lambda\lambda'})|a\rangle\Bigg\}.\end{aligned} \tag{4}$$

In the above, the time dependence of various operators appear while manipulating the cross section with the use of the Heisenberg representation when summing over the states $\{|b\rangle\}$. This expression can then be expressed in terms of correlation functions of various types,[13] $\chi_{o,o}$, $\boldsymbol{\chi}_{o,p}$, $\boldsymbol{\chi}_{o,s}$, $\boldsymbol{\chi}_{p,o}$ $\boldsymbol{\chi}_{s,o}$, $\boldsymbol{\chi}_{pp}$, $\boldsymbol{\chi}_{s,s}$, $\boldsymbol{\chi}_{s,p}$, and $\boldsymbol{\chi}_{p,s}$; the first one corresponds to the scalar correlation of the charge densities; the next two correspond to vector correlation functions associated with the charge density and vector momentum density and vector spin-density correlations; the next two are similar vector correlations where the roles are reversed; and the last four are second-order tensor correlation functions associated with the two vector densities of momentum and spin:

$$\begin{aligned}\left.\frac{d^2\sigma}{d\Omega' dE}\right|_{\lambda\to\lambda'} &=\left[\frac{e^2}{mc^2}\right]^2\frac{1}{2\pi\hbar}\int_{-\infty}^{\infty}dt e^{-i\omega t}\Bigg\{\chi_{o,o}(\mathbf{K},t)(\hat{\boldsymbol{\varepsilon}}_{\lambda}\cdot\hat{\boldsymbol{\varepsilon}}_{\lambda'})^*(\hat{\boldsymbol{\varepsilon}}_{\lambda}\cdot\hat{\boldsymbol{\varepsilon}}_{\lambda'})+\frac{i\hbar\omega_k}{mc^2}\frac{i}{\hbar k^2}((\boldsymbol{\chi}_{o,p}(\mathbf{K},t)\times\mathbf{K})\cdot\mathbf{C}_{\lambda\lambda'})(\hat{\boldsymbol{\varepsilon}}_{\lambda}\cdot\hat{\boldsymbol{\varepsilon}}_{\lambda'})^*\\ &-\frac{i\hbar\omega_k}{mc^2}\frac{i}{\hbar k^2}\{\mathbf{C}^*_{\lambda\lambda'}\cdot[\mathbf{K}\times\tilde{\chi}_{p,o}(\mathbf{K},t)]\}(\hat{\boldsymbol{\varepsilon}}_{\lambda}\cdot\hat{\boldsymbol{\varepsilon}}_{\lambda'})-\frac{i\hbar\omega_k}{mc^2}(\boldsymbol{\chi}_{o,s}(\mathbf{K},t)\cdot\mathbf{B}_{\lambda\lambda'})(\hat{\boldsymbol{\varepsilon}}_{\lambda}\cdot\hat{\boldsymbol{\varepsilon}}_{\lambda'})^*+\frac{i\hbar\omega_k}{mc^2}\mathbf{B}^*_{\lambda\lambda'}\cdot\boldsymbol{\chi}_{s,o}(\mathbf{K},t)\\ &\times(\hat{\boldsymbol{\varepsilon}}_{\lambda}\cdot\hat{\boldsymbol{\varepsilon}}_{\lambda'})+\left(\frac{i\hbar\omega_k}{mc^2}\right)^2\frac{i}{\hbar k^2}\mathbf{C}^*_{\lambda\lambda'}\cdot(\mathbf{K}\times\boldsymbol{\chi}_{p,s}(\mathbf{K},t))\cdot\mathbf{B}_{\lambda\lambda'}+\left(\frac{i\hbar\omega_k}{mc^2}\right)^2\frac{i}{\hbar k^2}\mathbf{B}^*_{\lambda\lambda'}\cdot(\boldsymbol{\chi}_{s,p}(\mathbf{K},t)\times\mathbf{K})\cdot\mathbf{C}_{\lambda\lambda'}\\ &+\left(\frac{i\hbar\omega_k}{mc^2}\right)^2\frac{1}{\hbar^2k^4}\mathbf{C}^*_{\lambda\lambda'}\cdot(\mathbf{K}\times\boldsymbol{\chi}_{p,p}(\mathbf{K},t)\times\mathbf{K})\cdot\mathbf{C}_{\lambda\lambda'}-\left(\frac{i\hbar\omega_k}{mc^2}\right)^2\mathbf{B}^*_{\lambda\lambda'}\cdot\boldsymbol{\chi}_{s,s}(\mathbf{K},t)\cdot\mathbf{B}_{\lambda\lambda'}\Bigg\}.\end{aligned} \tag{5}$$

TABLE I. Various quantities appearing in Eq. (5) for different configurations of incident and scattered (top) linearly and (bottom) circularly polarized light.

Configuration	$\hat{\boldsymbol{\varepsilon}}_\lambda \cdot \hat{\boldsymbol{\varepsilon}}_{\lambda'}$	$\mathbf{B}_{\lambda\lambda'}$	$\mathbf{C}_{\lambda\lambda'}$
		Linear polarization	
$\hat{\boldsymbol{\varepsilon}}_\parallel \rightarrow \hat{\boldsymbol{\varepsilon}}'_\parallel$	$\cos 2\theta$	$\sin 2\theta \hat{\mathbf{U}}_2$	$-\sin 2\theta \hat{\mathbf{U}}_2$
$\hat{\boldsymbol{\varepsilon}}_\parallel \rightarrow \hat{\boldsymbol{\varepsilon}}'_\perp$	O	$2\sin^2\theta(\sin\theta\hat{\mathbf{U}}_3 - \cos\theta\hat{\mathbf{U}}_1)$	$(\cos\theta\hat{\mathbf{U}}_1 + \sin\theta\hat{\mathbf{U}}_3)$
$\hat{\boldsymbol{\varepsilon}}_\perp \rightarrow \hat{\boldsymbol{\varepsilon}}'_\parallel$	O	$2\sin^2\theta(\sin\theta\hat{\mathbf{U}}_3 + \cos\theta\hat{\mathbf{U}}_1)$	$(-\cos\theta\hat{\mathbf{U}}_1 + \sin\theta\hat{\mathbf{U}}_3)$
$\hat{\boldsymbol{\varepsilon}}_\perp \rightarrow \hat{\boldsymbol{\varepsilon}}'_\perp$	1	$\sin 2\theta \hat{\mathbf{U}}_2$	O
		Circular polarization	
$\hat{\boldsymbol{\varepsilon}}_R \rightarrow \hat{\boldsymbol{\varepsilon}}'_R$	$-\sin^2\theta$	$2i\sin^3\theta\hat{\mathbf{U}}_3$	$\sin\theta(-\cos\theta\hat{\mathbf{U}}_2 + i\hat{\mathbf{U}}_3)$
$\hat{\boldsymbol{\varepsilon}}_R \rightarrow \hat{\boldsymbol{\varepsilon}}'_L$	$\cos^2\theta$	$\sin 2\theta(\hat{\mathbf{U}}_2 + i\sin\theta\hat{\mathbf{U}}_1)$	$-\cos\theta(\sin\theta\hat{\mathbf{U}}_2 + i\hat{\mathbf{U}}_1)$
$\hat{\boldsymbol{\varepsilon}}_L \rightarrow \hat{\boldsymbol{\varepsilon}}'_R$	$\cos^2\theta$	$\sin 2\theta(\hat{\mathbf{U}}_2 - i\sin\theta\hat{\mathbf{U}}_1)$	$-\cos\theta(\sin\theta\hat{\mathbf{U}}_2 - i\hat{\mathbf{U}}_1)$
$\hat{\boldsymbol{\varepsilon}}_L \rightarrow \hat{\boldsymbol{\varepsilon}}'_L$	$-\sin^2\theta$	$-2i\sin^3\theta\hat{\mathbf{U}}_3$	$-\sin\theta(\cos\theta\hat{\mathbf{U}}_2 + i\hat{\mathbf{U}}_3)$

We have thus expressed the cross section for scattering of light by a magnetic system in terms of the Fourier transforms of the various time-dependent correlation functions. In this form, the complete dynamical as well as spatial information concerning the effects of many-particle interactions within the system are included and thus an experimental determination of the cross section would contain complete information about the system. Theoretically these must be calculated in detail, as in Ref. 13, for example. For a paramagnetic system such as bulk Li metal, the expression containing only the last term given in Eq. (5) including spin-spin correlation was reported in Ref. 14. The effect of electron interactions in Li metal was incorporated in evaluating this spin-spin correlation function within random-phase approximation (RPA). We may evaluate the quality of the approximations made in theoretical calculations such as RPA by a comparison with the experimental results. We note that for magnetic systems of the types we are interested in bulk itinerant magnetic metals, Eq. (5) contains all possible spin contributions and as such is a completely general expression for scattering from magnetic systems and is thus more appropriate to use. The effects of electron interactions within the system must then be incorporated when evaluating the various correlation functions by employing techniques of many-particle theory as stated above.

A few comments on the significance of Eq. (5) may be in order. Our interest here is the experimental determination of magnetism of clusters of atoms. keV energy x rays from a synchrotron radiation source may be too energetic to probe properties of the cluster. We therefore approach this problem by optical spectroscopic methods, whose accuracy today may suffice for our purposes, as we will argue here. For typical laser wavelengths of the order of $(5-6)\times 10^{-5}$ cm used in modern spectroscopy, we find $(\hbar\omega/mc^2)\approx(5-4)\times 10^{-6}$. In magnetic clusters of Mn_5, according to Ref. 7, magnetization of the cluster is estimated to be $25\mu_B$, and is almost twice this in a Mn_{10} cluster. Thus the interference terms in Eq. (5) would be of the order of 10^{-4}. By including resonance contribution involving the states lying close to the highest occupied molecular orbital (HOMO) state and the lowest unoccupied molecular orbital (LUMO) state of the cluster, we may estimate a further factor $\hbar\omega/\Gamma \approx 10$, leading to an estimate of the cross section to be of the order of 10^{-6}.

Experimentally, one measures the ratio

$$\Delta R/R = (R_1 - R_2)/(R_1 + R_2), \tag{6}$$

where R_i (proportional to the cross section) stands for the intensity of specularly reflected light for a chosen configuration i of the incident and reflected polarizations of light, as given in Table I which is set up using the convention of Blume and Gibbs[3] as shown in Fig. 1. Often one chooses two configurations such that the difference in the numerator contains the information about the important features of the system under consideration. Experimentally, this is achieved through the use of near normal incidence reflection. There are two separate schemes that achieve the desired result. In the first case one uses polarizers on the incident and reflected branches of the optical bench. The polarizations are orthogonal to each other and hence will only measure a signal if sample has a preferred polarization. The sensitivity of this method is ultimately determined by the extinction ratio of the polarizers, which is 10^{-5} for high quality components.

A more elegant method of detecting polarization differences is based on the reflectance difference anisotropy technique that is commonly used in the study of semiconductor growth by molecular-beam epitaxy or chemical vapor deposition.[15] These techniques involved a polarization modulator which is either a rotating analyzer or a photoelastic modulator (PEM). The common idea is to periodically change the state of the polarization between the two orthogonal components and to use phase sensitive detection to extract the differences as shown in Eq. (6). The rotating analyzer system is limited to linear polarizations, while the photoelastic modulator based system can measure both linear[15] and circular dichroism.[16] These techniques are capable of detecting the linear polarization anisotropy of less than $\frac{1}{6}$ of a monolayer of Ga deposited on a viscinal surface of Si.[17] In these experiments, values of $\Delta R/R$ of order 10^{-5} were easily detected. It is believed that at least an order-of-magnitude improvement over this is possible. This would place the sensitivity within the range required to detect the magnetization in the clusters.

In Eq. (5), we note that the largest contribution to the cross section arises from the Thomson scattering from the charge distribution which is not our primary interest here.

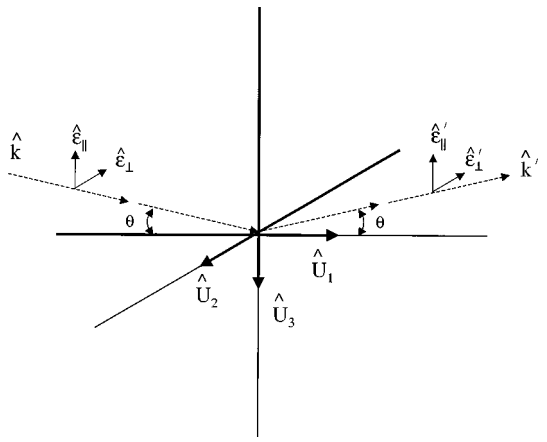

FIG. 1. The scattering geometry of Blume and Gibbs (Ref. 3). $\hat{\mathbf{k}},\hat{\mathbf{k}}'$ are the incident and the scattered wave vectors with 2θ, the scattering angle. $\hat{\boldsymbol{\varepsilon}}_{\perp}$ and $\hat{\boldsymbol{\varepsilon}}_{\parallel}$ are the components of the polarization perpendicular and parallel to the diffraction plane spanned by $\hat{\mathbf{U}}_1 = (\hat{\mathbf{k}}+\hat{\mathbf{k}}')/2\cos\theta$, $\hat{\mathbf{U}}_2 = (\hat{\mathbf{k}}\times\hat{\mathbf{k}}')/\sin 2\theta$, $\hat{\mathbf{U}}_3 = (\hat{\mathbf{k}}-\hat{\mathbf{k}}')/2\sin\theta$. With this, we have $\hat{\boldsymbol{\varepsilon}}_{\parallel} = \sin\theta\hat{\mathbf{U}}_1 - \cos\theta\hat{\mathbf{U}}_3$, $\hat{\boldsymbol{\varepsilon}}_{\perp} = -\hat{\mathbf{U}}_2$, $\hat{\boldsymbol{\varepsilon}}'_{\parallel} = (\sin\theta\hat{\mathbf{U}}_1 + \cos\theta\hat{\mathbf{U}}_3)$, $\hat{\boldsymbol{\varepsilon}}'_{\perp} = -\hat{\mathbf{U}}_2$.

The rest of the terms contain information about the spin and momentum distributions in the system and occur in two forms, four terms proportional to $(\hbar\omega/mc^2)\langle S\rangle$ arising from interference between charge and spin/momentum terms, and four others proportional to $[(\hbar\omega/mc^2)\langle S\rangle]^2$ due to spin/momentum terms. From Eq. (6) we observe that there are three possible types of configurations: (i) both numerator and denominator contain the Thomson contribution, (ii) both numerator and denominator do not contain charge contributions, and (iii) the numerator does not and the denominator has Thomson contribution. From Table I we observe that for linear polarization, the first and the last polarization configurations are of type (i) whereas the middle pairs are of type (ii). For circularly polarized light, the first and the last or the middle two, are both of type (iii), thus focusing on the spin contributions of our interest. Furthermore, in an experiment involving circular polarization the linear $\{(\hbar\omega/mc^2)\langle S\rangle\}$ interference terms contribute whereas in the linear polarization in type (ii) configuration would involve the quadratic $\{[(\hbar\omega/mc^2)\langle S\rangle]^2\}$ terms only.

Additionally, calculations[7] show that the electronic states of the Mn_x clusters are such that the HOMO to LUMO separation is about 2–3 eV. Furthermore, the LUMO levels for $x=3,4$ are nearly degenerate pairs of states. This opens up the possibility of performing visible-light spectroscopy of the clusters and obtaining specific information about their electronic structure, because the electronic structure is different for different spin states and different cluster sizes (x). Therefore reflectance difference spectroscopy would be very useful in completely understanding the clusters and their magnetization.

We thank Professor P. Jena for introducing us to the magnetism of clusters and providing us with preprints and reprints of Refs. 7 and 9. Professor S. D. Mahanti introduced one of us (A.K.R.) to the work of Blume and Gibbs in Ref. 3, on the determination of detailed magnetic structures using synchrotron radiation. We thank Dr. Sharka Prokes for many illuminating discussions on the experimental aspects of this work. M.M.'s visit to NRL was sponsored by the Navy/ASEE Summer Faculty Program, which is gratefully acknowledged. This work was supported in part by the Office of Naval Research.

[1] P. M. Platzman and N. Tzoar, Phys. Rev. B **2**, 3556 (1970).

[2] F. de Bergevin and M. Brunel, Acta Crystallogr., Sect. A: Cryst. Phys., Diffr., Theor. Gen. Crystallogr. **A37**, 314 (1981); M. Brunel and F. de Bergevin, *ibid.* **A37**, 324 (1981).

[3] M. Blume, J. Appl. Phys. **57**, 3615 (1985); M. Blume and Doon Gibbs, Phys. Rev. B **37**, 1779 (1988).

[4] E. Balcar and S. W. Lovesey, *Theory of Magnetic Neutron and Photon Scattering* (Clarendon Press, Oxford, 1989).

[5] R. S. Service, Science **271**, 920 (1996).

[6] J. Shi, S. Gider, K. Babcock, and D. D. Awschalom, Science **271**, 937 (1996).

[7] S. K. Nayak and P. Jena, Chem. Phys. Lett. **289**, 473 (1998); see also S. K. Nayak, B. K. Rao, and P. Jena, J. Phys. C (to be published); S. K. Nayak and P. Jena, J. Am. Chem. Soc. (to be published); Phys. Rev. Lett. **81**, 2970 (1998).

[8] M. Y. Lai and Y. L. Wang, Phys. Rev. Lett. **81**, 164 (1998).

[9] V. S. Stepanyuk, W. Hergret, K. Wildbeger, S. K. Nayak, and P. Jena, Surf. Sci. **384**, L892 (1997).

[10] J. L. Simmonds, Phys. Today **48** (4), 26 (1995); E. D. Dahlberg and J. G. Zhu, *ibid.* **48** (4), 34 (1995); D. D. Awschalom and D. P. DiVincenzo, *ibid.* **48** (4), 43 (1995); G. A. Prinz, *ibid.* **48** (4), 58 (1995).

[11] C. A. Baumann, R. J. Van Zee, S. V. Bhat, and W. Weltner, Jr., J. Chem. Phys. **78**, 190 (1983).

[12] A. Traverse, New J. Chem. **22**, 677 (1998).

[13] A. K. Rajagopal and M. Mochena, Phys. Rev. B **57**, 11 582 (1998).

[14] C. Petrillo and F. Sacchetti, Solid State Commun. **91**, 895 (1994).

[15] D. E. Aspnes, J. P. Harbison, A. A. Studna, and L. T. Florez, J. Vac. Sci. Technol. A **6**, 1327 (1988); D. E. Aspnes, in *Diagnostic Techniques for Semiconductor Materials Processing*, edited by O. J. Glembocki, S. W. Pang, F. H. Pollak, G. M. Crean, and G. Larrabee, MRS Symposia Proceedings No. 324 (Materials Research Society, Pittsburgh, 1994), p. 3, and references therein.

[16] L. A. Nafie and M. Diem, Appl. Spectrosc. **33**, 130 (1979).

[17] O. J. Glembocki and S. M. Prokes, Appl. Phys. Lett. **71**, 2355 (1997).